

Surface Modification of Nanoclay for the Synthesis of Polycaprolactone (PCL) – Clay Nanocomposite

Kamal Yusoh^{1,*}, Shamini Vesaya Kumaran¹, and Fadwa Sameeha Ismail¹

¹Faculty of Chemical and Natural Resources Engineering, Universiti Malaysia Pahang, 26300 Gambang, Pahang Malaysia

Abstract. This paper presents a new modification method to modify the surface of nanoclay (Na-MMT) to increase its *d*-spacing using Aminopropylisooctyl Polyhedral Oligomeric Silsesquioxane (AP-POSS) and the fabrication of Polycaprolactone (PCL) nanocomposite through solution intercalation technique. The structure and morphology of pure nanoclay, modified nanoclay (POSS-MMT) and the PCL nanocomposite were characterized by X-ray Diffraction (XRD), Fourier Transform Infrared Spectroscopy (FTIR) and Field Emission Scanning Electron Microscopy (FESEM). XRD revealed that the *d*-spacing of the POSS-MMT is increased by 0.64 nm as compared to pure nanoclay. FTIR and FESEM results also showed that AP-POSS were well dispersed and intercalated throughout the interlayer space of Na-MMT. An exfoliated structure was also observed for PCL/POSS-MMT nanocomposite. Thermal properties of the nanocomposite were investigated using Thermal Gravimetry Analysis (TGA) which recorded highest degradation temperature for PCL/POSS-MMT 1% nanocomposite which is 394.1°C at 50% weight loss ($T_{50\%}$) but a decrease in degradation temperature when POSS-MMT content is increased and Differential Scanning Calorimetry (DSC) analysis which showed highest melting and crystallization temperature for PCL/POSS-MMT 5% nanocomposite which is 56.6°C and 32.7°C respectively whereas a decrease in degree of crystallinity for PCL/POSS-MMT nanocomposite as compared to PCL/Na-MMT nanocomposite. This study affords an efficient modification method to obtain organoclay with larger interlayer *d*-spacing to enhance the properties of polymer nanocomposite.

1 Introduction

Plastics are ideal for many applications such as in packaging, building materials and commodities but it can lead to waste disposal problems. Accumulation of plastic at the end of its life cycle had increased drastically on the earth causing serious pollution problems. Therefore, this motivated many researchers to conduct studies to produce a biodegradable and environmental friendly polymer nanocomposite to produce plastics. There has been a strong emphasis in the development of polymer nanocomposites for the last 20 years. Polymer nanocomposites consist of inorganic nanofiller and organic polymers represent a new class of materials that exhibit improved performance compared to their microcomposite counterparts [1].

Polycaprolactone (PCL) is considered to be a good biodegradable polymer because of the low production cost and easy processibility in large scale production. PCL have good commercial potential for plastics but their low thermal and mechanical properties for further processing restrict their use in a wide range of applications [2]. Therefore, these properties can be improved through the preparation of PCL nanocomposite by incorporating nanofiller such as nanoclay.

Sodium montmorillonite (Na-MMT) is the most abundant nanoclay mineral that is easily available with a good swelling capacity, high cation exchange capacity and high surface area [3]. However, the hydrophilic nature of nanoclay hinders homogenous dispersion of nanoclay in the hydrophobic polymer matrix [4]. Modifying the nanoclay surface through organic treatment will give a hydrophobic environment to the galleries of the Na-MMT and enhance its compatibility with the polymer matrix. Conventional modification method is the ion-exchange reaction using cationic salts such as alkyl ammonium or phosphonium salts. There are some drawbacks in this modification process such as low thermal stability of the cationic salts and the compounds are less readily intercalated in the polymer melts. Alkyl ammonium salt will decompose at temperature above 170-180°C which shows that it is not suitable for the high temperature melt processing techniques [5].

Thus, a new modification method will be the main aim of this study. The surfactant method by using Aminopropylisooctyl Polyhedral Oligomeric Silsesquioxane (AP-POSS) is developed to give a better surface modification for the Na-MMT. The main

* Corresponding author: kamal@ump.edu.my

purpose of the surface modification of Na-MMT is to expand the interlayer *d*-spacing of the nanoclay gallery so that polymer molecules can penetrate as well as to enhance its miscibility with polymer to achieve a good dispersion. AP-POSS has a high thermal stability which is up to 300°C. Therefore, an enhanced PCL nanocomposite can be produced with modified nanoclay.

Polymer nanocomposites usually can be prepared by using three different techniques such as in-situ polymerisation, melt blending and solution intercalation. Solution intercalation method is considered in this study because only a small amount of polymer nanocomposite is to be fabricated in a laboratory scale whereas the other two techniques is preferred for industrial scale. Thus, the main aim of this study is to develop a new modification method for dispersing nanofillers in PCL nanocomposite and to fabricate PCL nanocomposite through solution intercalation technique.

2 Experimental

2.1. Materials

Sodium montmorillonite (Na-MMT) was purchased from Southern Clays, Texas, US. The organic modifier, Aminopropylisooctyl Polyhedral Oligomeric Silsesquioxane (AP-POSS) was purchased from Hybrid Plastic Co., USA. Polycaprolactone (PCL), ethanol, acetic acid and chloroform were purchased from Fisher Scientific.

2.2 Modification of Na-MMT using Surfactant Method

Five (5) g of Na-MMT was suspended in 250 ml of deionised water at 25°C with stirring for 2 hours. 2.332 g of AP-POSS was dissolved in 6 ml of ethanol and acidified with 4 ml of acetic acid. It is then added dropwise to the Na-MMT suspension over a period of 20 min [6]. The mixed suspension was then continuously stirred at 70°C for 24 hours to obtain the organoclay (POSS-MMT). Then the organoclay was harvested by centrifuge, dried in oven for 48 hours and ground to pass mesh sieve.

2.3 Fabrication of PCL Nanocomposite

The nanoclay (1wt%, 3wt% and 5wt%) was stirred in chloroform for $1\frac{1}{2}$ hours. PCL (1g) was also stirred with chloroform (20ml) to get a solution of PCL/Chloroform. That solution was then dropped into nanoclay/chloroform suspension and stirred for $4\frac{1}{2}$ hours. The suspension was poured into a clean petri dish and left covered for 2 days. After 2 days, the film was dried in a vacuum oven for 24 hours at 40°C to remove the residual traces of chloroform.

2.3 Fabrication of PCL Nanocomposite

XRD data was recorded on a MiniFlex Rigaku using graphite-filtered Cu-K α radiation (1.25, 0.154 nm). The diffractometer was controlled using Diffrac Plus XRD Commander and the raw data was manipulated using EVA software [6]. All the data were collected between the ranges of 3° to 80° 2 θ with a resolution of 0.02°. The *d*-spacing of the nanoclay were calculated by using the Bragg's law.

$$\sin \theta = n\lambda / 2d \quad (1)$$

Where, *d* is the spacing between the layers of the nanoclay, λ is the wavelength of the X-Ray which is 0.154 nm, θ is the angle at the maximum point of the first peak in the spectra, *n* is the order of diffraction which 1.

FTIR was recorded by using Nicolet Omnic 3 FTIR spectrophotometer. The samples were used in the solid form. The background of the samples was in KBr standard. After the background is completed, the reading for the samples was collected.

FESEM analysis was done by using the JEOL FESEM JSM-7100F. 'Smart FESEM User Interface' program was run. The samples were mounted on the universal holder with stub forceps. The focus knob was turned to sharp the scanned images. FESEM images then were saved.

2.4 Thermal Analysis of PCL nanocomposite

TGA analysis was carried out by using Perkin Elmer TGA Q500. The samples were heated from 25°C to 600°C at a heating rate of 5°C/min under nitrogen atmosphere. A mass change versus temperature curve was obtained.

DSC analysis was done using Perkin Elmer DSC Q1000 under nitrogen atmosphere. Measurement was performed from room temperature to 160°C at heating rate of 10°C/min. The samples were stand stilled for 5 minutes to erase any previous thermal history. Subsequent cooling and heating cycles was recorded respectively. The degree of crystallinity (X_{cr}) of the sample was calculated by using equation shown below.

$$X_{cr} (\%) = (\Delta H_f) / (W_{PCL} \times \Delta H_{100}) \times 100\% \quad (2)$$

ΔH_{100} represents heat of fusion of 100% crystalline PCL [136.1 J/g [7]], ΔH_f represents experimental heat of fusion and W_{PCL} represents weight fraction of PCL.

3 Results and Discussion

3.1 Characterization of Nanoclay

X-ray Diffraction (XRD) analysis was used to characterize the interlayer *d*-spacing of the nanoclay galleries and the dispersion of nanoclay in the polymer nanocomposite structure. The pure nanoclay, Na-MMT shows the first characteristic peak at $2\theta = 14.9^\circ$ and the modified nanoclay, POSS-MMT shows at $2\theta = 7.16^\circ$ as indicated in the **Figure 1**. It can be clearly observed that

there is a shift of characteristic reflections to lower angle in POSS-MMT compared to Na-MMT. The *d*-spacing of the nanoclays were calculated by using EQN 1. The *d*-spacing of the nanoclays increased from 0.593 nm for Na-MMT to 1.233 nm for POSS-MMT. This proved that the AP-POSS surfactant was successfully intercalated into the nanoclay galleries consequently pushing the nanoclay layers and confirms that modification process has taken place. Thus, this result corresponds to the study conducted by Zhao *et al.* (2009) [8] where the *d*-spacing of the nanoclays increased from 0.96 nm for Na-MMT to 1.25 nm for POSS-MMT. This intercalation is an efficient way to increase the material surface hydrophobicity of Na-MMT which is a fundamental requirement for good compatibility between the polymer matrix and the Na-MMT surface [9]. Surfactant method gives a better increase in the *d*-spacing of the nanoclay compared to ion exchange reaction by alkyl ammonium salts where in the studies conducted by Uhl *et al.* (2004) [10], cetyltrimethylammonium bromide (CTMA) increases the nanoclay galleries only by 0.5 nm while the surfactant method used in this study could increase the nanoclay layer by 0.64 nm.

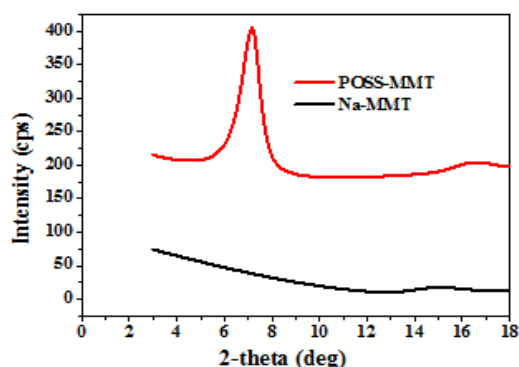


Fig. 1. XRD Spectra for Na-MMT and POSS-MMT

Fourier Transform Infrared Spectroscopy (FTIR) was used to analyse the presence of certain functional group in a molecule. In Figure 2, Na-MMT shows characteristic peak at 3630.97 cm^{-1} which represents the hydroxyl stretching vibration of OH group and at 3460.63 cm^{-1} which represents the broad band of stretching vibration of the interlayer water. Na-MMT also exhibits strong peaks at 1045.79 cm^{-1} for the Si-O stretching vibration, 523.87 cm^{-1} for the Al-O-Si deformation and 466.81 cm^{-1} for Si-O-Si deformation bonds [11]. The H-O-H bending vibration band can be observed at 1639.14 cm^{-1} . All these bands are also present in POSS-MMT. The AP-POSS surfactant exhibits characteristic absorption peak for its aliphatic C-H stretching vibration from CH_2 groups at 3000-2800 cm^{-1} . The stretching vibration of N-H bond also might be present in the same band. AP-POSS also shows a peak at 1226.37 cm^{-1} for Si-C bond [12]. The symmetrical Si-O-Si bond in the silsesquioxane cage is at stretching band of 1092.76 cm^{-1} [12]. All these bands also can be observed in the POSS-MMT which indicates the intercalation of AP-POSS surfactant into the nanoclay

galleries. After the intercalation of AP-POSS surfactant, POSS-MMT not only had the characteristic bands of Na-MMT but also exhibited the characteristic bands of AP-POSS surfactant.

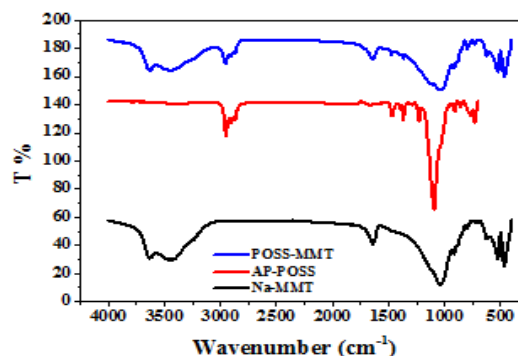
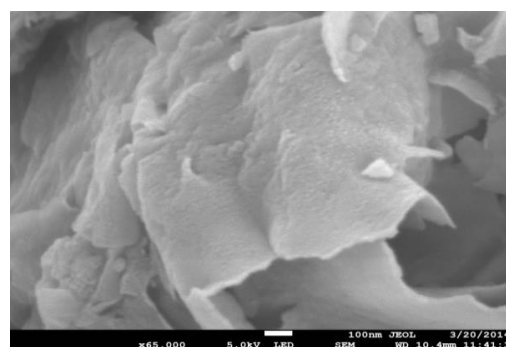
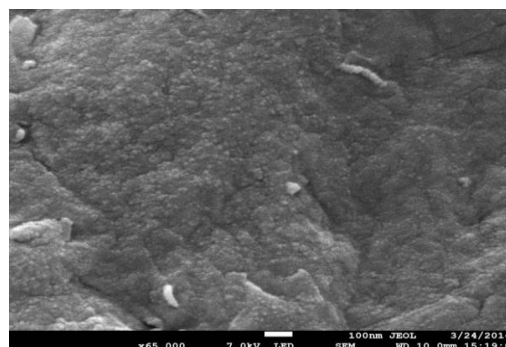


Fig. 2. FTIR Spectra for Na-MMT, AP POSS and POSS-MMT

The morphology of Na-MMT and POSS-MMT were analysed by means of FESEM. Figure 3 shows the FESEM images for both the nanoclays. In Figure 3 (a), the Na-MMT shows aggregated and curved plates. It also has a number of flakes with severely crumpled structure. In Figure 3 (b), POSS-MMT shows a finer and uniform morphology. The aggregated, curved and crumpled structure of the Na-MMT disappears and well dispersed particles obtained after modification. Finer and more uniform morphology is obtained in the modified nanoclay. This result is speculated might be because of the well intercalated nanoclay galleries with increased *d*-spacing which are due to the modification by using AP-POSS.



3(a)



3(b)

Fig. 3. FESEM images of nanoclay (a) Na-MMT and (b) POSS-MMT

3.1 Characterization of PCL Nanocomposites

XRD traces for the POSS-MMT and PCL/POSS-MMT nanocomposite is shown in **Figure 4**. The POSS-MMT has a characteristic peak at 2θ of 7.16° , corresponding to interlayer d -spacing of 1.233 nm. There are no visible peaks for PCL/POSS-MMT nanocomposite which validates the formation of an exfoliated structure in the nanocomposite. The octyl chains in AP-POSS will be in straight alignment position by pushing the nanoclay interlayer galleries after the modification and PCL chains enter into the interlayer galleries of the nanoclay. This occurrence might have caused the destruction of the ordered geometry of nanoclay and resulting in complete delamination of the nanoclay layer on PCL matrix and forms an exfoliated structure. Similar observation has been reported by Liu *et al.* (2005) [13] where epoxy nanocomposite fabricated with POSS-modified MMT does not exhibit any diffraction peaks in the XRD pattern representing exfoliated structure.

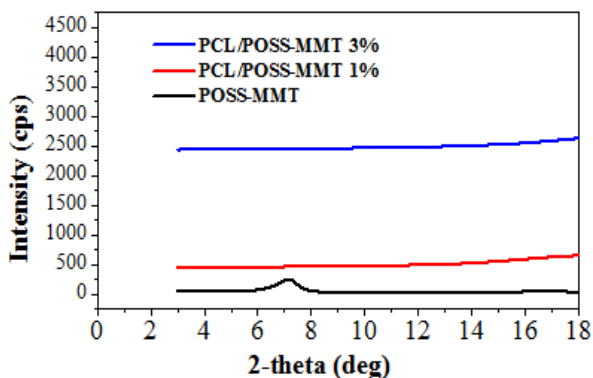


Fig. 4. XRD Pattern for POSS-MMT and PCL/POSS-MMT Nanocomposite

The FTIR spectra for pure PCL and PCL nanocomposite samples are shown in **Figure 5**. The pure PCL have peaks located at $2930\text{-}2945\text{ cm}^{-1}$ representing CH_2 bonds stretching vibration. The vibration of $\text{C}=\text{O}$ bonds present at 1724 cm^{-1} band. The region of 1275 cm^{-1} to 1050 cm^{-1} indicates the $\text{C}-\text{O}-\text{C}$ aliphatic ether stretching vibrations. All these important characteristic bands are situated in each PCL nanocomposite structure and show the presence of PCL. A new characteristic peak can be observed at the region of $3470\text{-}3485\text{ cm}^{-1}$ in the entire PCL nanocomposites. These peaks represent the broad band of stretching vibration of the interlayer water in the Na-MMT silicate. This band shows a slight increase in its intensity correlated with the increasing nanoclay content in each nanocomposite samples [14]. The most intense characteristic bands for Na-MMT are located in the region $1050\text{-}990\text{ cm}^{-1}$ attests the $\text{Si}-\text{O}$ stretching vibrations. Unfortunately, those characteristic bands cannot be distinguished because PCL has multiple bands in the same IR spectral range [14]. The presence of important principal characteristic bands of POSS-MMT falls in the region between 3000 cm^{-1} to 2800 cm^{-1} . These bands which represent the CH_2 stretching vibration and the $\text{N}-\text{H}$ bonds are also present in the pure

PCL structure. It also can be seen a small increase in the intensity of that particular peaks with increasing POSS-MMT content. This result clearly verifies that intercalation of PCL with both unmodified and modified nanoclay has occurred.

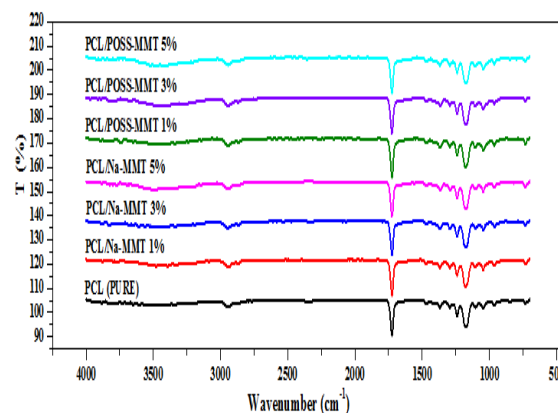
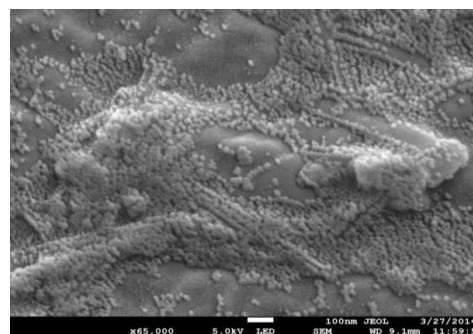
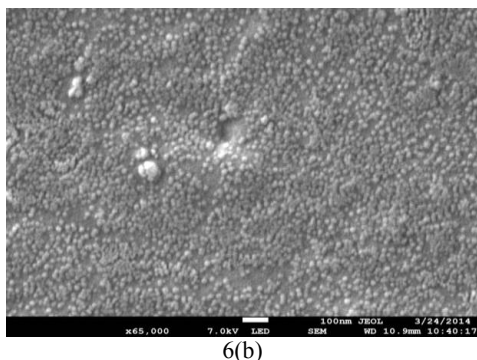


Fig. 5. FTIR Spectra of Pure PCL and PCL Nanocomposite

The FESEM analysis for PCL nanocomposite shows that POSS-treated nanoclay nanocomposite gives a matrix with well distributed particles compared to pure nanoclay nanocomposite as shown in **Figure 6**. In PCL/Na-MMT nanocomposite, nanoclay tends to stack together and do not disperse uniformly in the PCL matrices as shown in **Figure 6(a)**. The Na-MMT tends to be agglomerated and stacked on the PCL matrix. This is because the immiscibility between Na-MMT and PCL is a major issue due to poor interfacial adhesion [15]. The distribution of modified nanoclay layers in PCL/POSS-MMT nanocomposite appeared more uniform throughout the polymer matrix. The difference in morphology of PCL/Na-MMT 5% and PCL/POSS-MMT 5% nanocomposite is very obvious where the agglomerated particles disappear completely in PCL/POSS-MMT 5% nanocomposite as shown in **Figure 6(b)**. This occurrence of finely dispersed modified nanoclay throughout the entire PCL matrix is because the compatibility of Na-MMT and PCL has been increased by modifying the Na-MMT.



6(a)



6(b)

Fig. 6. FESEM images for PCL nanocomposite (a) PCL/Na-MMT (5%) and PCL/POSS-MMT (5%)

Thermal degradation of pure PCL and PCL nanocomposite was monitored through TGA. PCL materials degrade with a large peak in single step as observed for each sample in **Figure 7**. The degradation temperatures for 50% weight loss ($T_{50\%}$) decreases gradually from 392.9°C for pure PCL to 391.4°C for PCL/Na-MMT 5% nanocomposite and this is due to the incompatibility of Na-MMT with PCL matrix together with its hydrophilic character which can be related to the decomposition of physically adsorbed water and water molecules surrounding the exchangeable sites in Na-MMT. A noticeable increase in degradation temperature at $T_{50\%}$ can be observed for PCL/POSS-MMT 1% nanocomposite which is 394.1°C. The shift to higher degradation temperature is because POSS-MMT may act as a mass transport barrier to the volatile product that is generated during decomposition or diffusion hindrance of the decomposed volatiles through nanocomposite [16]. In a study conducted previously, the degradation temperature was higher for PCL/MMT- C_8H_{17} nanocomposite and lower for PCL/Na-MMT nanocomposites compared to neat PCL at $T_{50\%}$ [16]. PCL/POSS-MMT 3% and 5% nanocomposite have the lowest degradation temperature among other samples which is 382.3°C and 364.8°C respectively. This can be associated with two major effects as the content of POSS-MMT increased. Firstly, the POSS-MMT could have functioned as an inorganic catalyst for polymer degradation [17]. Secondly, the AP-POSS surfactant can be decomposed at lower temperatures following the Hoffman elimination where these resulting degradation products of AP-POSS could have possibly contributed in catalyzing the degradation of PCL matrix [9]. The resistance to thermal degradation was improved when the organically modified nanoclay content is 1 wt% in PCL matrix but the effect levels off independently of the modified nanoclay beyond that content [16]. Thus, the results obtained becomes obvious that the modified nanoclay may possess two opposing functions in thermal stability of polymer nanocomposites where it improves the thermal stability by barrier effect and decreases the thermal stability by catalytic effect on the degradation of the polymer matrix.

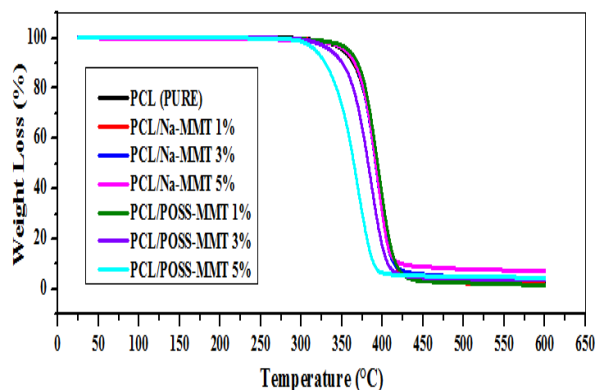


Fig. 7. TGA curves of Pure PCL and PCL Nanocomposite

The effect of nanoclay on the melting temperature (T_m), crystallization temperature (T_c) and degree of crystallinity (X_{cr}) of PCL was analysed by DSC. Based on **Table 1**, it can be clearly seen that PCL/POSS-MMT nanocomposites possess a higher T_m compared to PCL/Na-MMT nanocomposite loaded with equal amount of nanoclay and pure PCL where it shows 56.6°C for PCL/POSS-MMT 5% nanocomposite. In the case of T_c , the PCL/Na-MMT nanocomposite experiences a decrease in the T_c from pure PCL to PCL/Na-MMT 5% nanocomposite which is from 31.9°C to 31.0°C then increases when POSS-MMT is incorporated into the PCL which is up to 32.7°C for PCL/POSS-MMT 5% nanocomposite. Similar results were reported by Di *et al.* (2003) [18], where T_c of the polymer matrix increased with the addition of a small amount of C30B, an organoclay to the PCL matrix. The increase in both these temperatures are because of increased order of lamellar crystals of PCL or the molecular mobility of PCL segments was suppressed by spatial confinement due to the presence of organoclay particles [19]. There also could be nano-reinforcement effect of Na-MMT layers together with the intercalating AP-POSS surfactant which were well dispersed in the PCL matrix. The T_m and T_c of nanocomposite depend on the degree of dispersion of nanoclay and its dispersed sizes in the polymer matrix. The PCL/Na-MMT nanocomposites have a higher X_{cr} (calculated by equation 2) compared to the PCL/POSS-MMT nanocomposite with the same amount of nanoclay loading. The presence of surfactant at the interface can prevent the nucleation process and leads to decrease in the crystallinity [20]. The decrease in X_{cr} is also due to the reduced mobility of the polymer chains in presence of strongly interacting nanoclay [18]. Thus, incorporation of modified nanoclay into PCL matrix improves the T_m and T_c compared to unmodified nanoclay but reduces the X_{cr} .

Table 1. DSC Data for Pure PCL and PCL Nanocomposite

Sample	Melting Temperature (°C)	Crystallization Temperature (°C)	Degree of Crystallinity (%)
PCL (Pure)	55.9	31.9	33.6
PCL/Na-MMT 1%	56.4	31.5	40.9
PCL/Na-MMT 3%	56.3	30.6	43.8
PCL/Na-MMT 5%	56.3	31.0	40.2
PCL/POSS-MMT 1%	56.5	31.8	37.3
PCL/POSS-MMT 3%	56.4	32.2	37.2
PCL/POSS-MMT 5%	56.6	32.7	35.8

4 Conclusion

The new AP-POSS based surfactant method for modification of nanoclay was done successfully where a significant increase in the interlayer *d*-spacing from 0.593 nm in Na-MMT to 1.233 nm in POSS-MMT has been achieved. The AP-POSS surfactant was successfully intercalated into the interlayer galleries of Na-MMT. The disappearance of diffraction peak in XRD for PCL/POSS-MMT nanocomposite and FESEM images verifies a good dispersion of POSS-MMT layers in the PCL matrix. TGA results showed highest degradation temperature of 394.1°C at T_{50%} for PCL/POSS-MMT 1% nanocomposite. DSC data showed highest T_m of 56.6°C and T_c of 32.7°C for PCL/POSS-MMT 5% nanocomposite with a lower X_{cr} of 35.8% as compared to PCL/Na-MMT nanocomposite. PCL/POSS-MMT nanocomposite has enhanced thermal properties compared to pure PCL. Organic modification of nanoclay with new surfactant method gives good potential for incorporation with various biodegradable polymers such as Polybutylene Succinate and Poly(lactic Acid) to give enhanced properties.

The authors gratefully acknowledge the financial supported by UMP under research funding RDU150398 and Ministry of Higher Education Malaysia under FRGS scheme RDU160149

References

- Kango, S., Kalia, S., Celli, A., Njuguna, J., Habibi, Y., & Kumar, R. (2013). *Progress in Polymer Science*, 38, 1232–1261.
- Sinha, R.S.S., & Bousima, M. (2005). *Prog. Mater. Sci.*, Vol. 50, 962–1079
- Hossain, M. D., Kim, W. S., Hwang, H. S., & Lim, K. T. (2009). *Journal of Colloid and Interface Science*, 336, 443–448.

- Gorrasi, G., Tortora, M., Vittoria, V., Pollet, E., Lepoittevin, B. D., Alexandre, M., & Dubois, P. (2003). *Polymer*, 44, 2271–2279.
- Sarier, N., Onderb, E., & Ersoyb, S. (2010). *Colloids and Surfaces A: Physicochem. Eng. Aspects*, 371, 40–49.
- McLauchlin, A., Bao, X., & Zhao, F. (2011). *Applied Clay Science*, 53, 749-753.
- Yam, W. Y., Ismail, J., Kammer, H. W., Schmidt, H., & Kummerlowe, C. (1999). *Polymer* 40, 5545–5552.
- Zhao, F., Wan, C., Bao, X., & Kandasubramanian, B. (2009). *Journal of Colloid and Interface Science*, 333, 164–170.
- Achaby, M. E., Ennajih, H., Arrakhiz, F.Z., Kadib, A. E., Bouhfid, R., Essassi, E., & Qaiss, A. (2013). *Composites: Part B*, 51, 310–317.
- Uhl, F. M., Davuluri, S. P., Wong, S. C., & Webster, D. C. (2004). *Polymer*, 45, 6175–6187.
- Zhou, Q., Pramoda, K. P., Lee, J. M., Wang, K., & Loo, L. S. (2011). *Journal of Colloid and Interface Science*, 355, 222–230.
- Fu, H. K., Kuo, S. W., Yeh, D. R., & Chang, F. C. (2008). *Journal of Nanomaterials*, Article ID 739613, 7 pages.
- Liu, H. Z., Zhang, W., & Zheng, S. (2005). *Polymer*, 46, 157–65.
- Viville, P., & Lazzaroni, R. (2003). *Langmuir*, 19, 9425-9433.
- Ahmed, J., Auras, R., Kijchavengkul, T., & Varshney, S. K. (2012). *Journal of Food Engineering*, 111, 580–589.
- Lepoittevin, B., Pantoustier, N., Alexander, M., Calberg, C., Jerome, R., & Dubois, P. (2002). *J Mater Chem*, 12, 3528–32.
- Qin, H., Zhang, S., Zhao, C., Feng, M., Yang, M., Shu, Z., et al. (2004). *Polym Degrad Stabil*, 85, 807–13.
- Di, Y., Iannace, S., Maio, E. D., & Nicolais, L. (2003). *J Polym Sci Part B: Polym Phys*, 41, 670–8.
- Wu, T., Xie, T., & Yang, G. (2009). *Applied Clay Science*, 45, 105–110.
- Eleonora, E., Fernanda, M., Antonia, & T.M., Hugo, D. (2011). *Journals of Material Science and Engineering A*, 778-789.